

The effect of the die rotation during extrusion on the shape of embedded markers

Mykola Kulakov^{a,*}, Matthias Mail^b, Roman Kulagin^b

^a Boeing Research and Technology – Europe, 85 Inchinnan Drive, Renfrew PA4 9LJ, United Kingdom

^b Institute of Nanotechnology, Karlsruhe Institute of Technology, 76344 Eggenstein-Leopoldshafen, Germany

ARTICLE INFO

Keywords:

Friction stir extrusion
High-pressure torsion extrusion
Computed tomography
Flow markers
Architected materials

ABSTRACT

The introduction of die rotation during extrusion changes the material flow pattern. An initially straight flow marker embedded into a billet to visualise plastic flow is twisted into a spiral during rotation-assisted extrusion in addition to the reduction in the cross-sectional area. Moreover, the shape of the marker as observed on two-dimensional sections perpendicular to the extrusion axis changes from a circle to a teardrop. A simple model was proposed to describe these changes. The method is based on two transformations to account for the grid pattern distortion during conventional extrusion without rotation and for the torsion due to the die rotation. A good agreement was obtained between calculations and experimentally observed marker shape changes during high-pressure torsion extrusion and previously reported results for friction stir extrusion.

1. Introduction

Several modifications of conventional extrusion exist whereby in addition to the axial pressure, a monotonic rotational operation is introduced. Examples of this type of processes include but not limited to high-pressure torsion extrusion (HPTE), shear extrusion (SE) (also known as torsion extrusion) and friction stir extrusion (FSE) (Fig. 1). Each of the processes possesses its own peculiarities.

During HPTE, one of the containers remains stationary while the other one rotates (Fig. 1(a)) [1,2]. Typical rotation speeds are ~ 1 rpm. Frictional forces between the extrudate and the rotating container are counterbalanced by that in the stationary container; when a sufficiently long specimen is extruded, the opposing frictional forces cause shear deformation in a narrow section between the two containers. A faceted design of the containers is typically used to minimise slippage between the extrudate and containers.

During SE, the extrudate simultaneously undergoes the cross-section reduction due to the axial pressure and torsional deformation under the action of the conical die rotating typically at below 10 rpm (Fig. 1(b)) [3–5]. Only a fraction of the rotational work is transmitted to the material due to slippage between the extrudate and the stationary container or the rotating die. Compared to the conventional extrusion process without rotation, a lower extrusion force during rotation-assisted extrusion is attributed to the change in the direction of the friction

stress and the superposition of axial and tangential stresses.

A rotating die is plunged into the material during FSE (Fig. 1(c)) [6,7]. The rotational speed of the tool can be as high as several hundred rpm. The process is conducted at an elevated temperature due to deformation heating thereby eliminating the need to preheat feedstock.

Markers are indispensable for the study of metal plastic flow during forming processes [8]. For example, based on changes in the position and shape of markers, discrete values of plastic strain can be estimated [9]. Alternatively, markers can be used to calibrate kinematically admissible velocity field and to calculate the distribution of strain [10]. For the processes discussed above, when a wire placed parallel to the extrusion axis is used as a flow marker, it is twisted into a spiral [1,11]. Moreover, the shape of the marker in a section perpendicular to the extrusion axis changes from a circle to a teardrop due to the die rotation. This effect is not observed during free end torsion or during conventional extrusion without rotation.

A simple methodology to calculate the shape of embedded flow markers during rotation-assisted extrusion is proposed in this study. The efficacy of the method was demonstrated for a billet containing multiple flow markers after HPTE and previously reported data for FSE [11].

2. Model describing marker shape transformations

Two operations are required to transform initial coordinates for any

* Corresponding author.

E-mail address: nkulako@gmail.com (M. Kulakov).

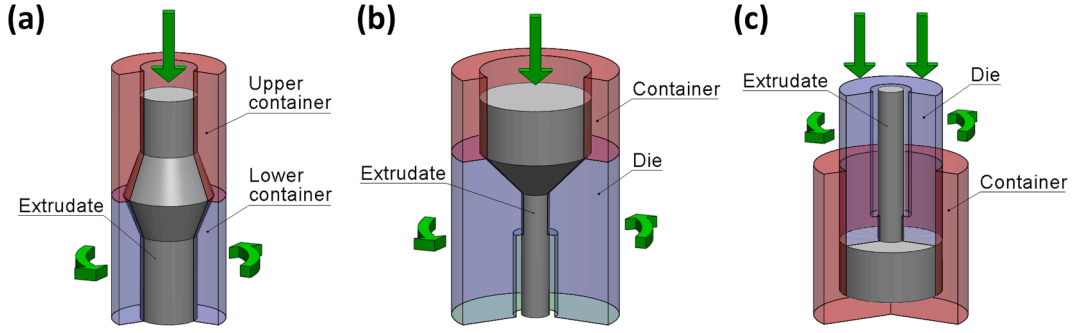


Fig. 1. Schematic diagram of (a) high-pressure torsion extrusion, (b) shear extrusion and (c) friction stir extrusion.

location before extrusion (x_0, y_0, z_0) to final coordinates (x_1, y_1, z_1) in the extrudate.

The first operation accounts for the characteristic grid distortion pattern observed during extrusion without die rotation [12]. A straight grid line drawn perpendicular to the extrusion axis is distorted in a such manner that central sections of the line are pulled forward in the direction of extrusion with respect to the ends of the line near the extrudate surface. Similarly, a two-dimensional section initially perpendicular to the extrusion axis rotates relative to the axis. For an extrudate having a circular cross-section, the first operation can be described using the following equation:

$$z_1 = z_0 + z_c \left(1 - \frac{r^n}{R_1^n} \right) \quad (1)$$

where z_c and n are adjustable parameters, r is the radius corresponding to the point (x_1, y_1, z_1) in the extrudate and R_1 is the radius of the extrudate.

The adjustable parameter z_c determines the extent of distortions of the extrudate cross section including that of any embedded markers in the direction parallel to the extrusion axis; for greater values of z_c , stretching of the marker will be more pronounced. As the parameter n influencing the distribution of distortions in the radial direction increases (above 1), markers located closer to the extrusion axis receive less distortion, while markers located near the periphery are more distorted.

The second operation is required to describe the change in coordinates introduced due to the die rotation. Simplistically, free end

torsion of a cylinder can be represented through a stack of thin sections rotating with respect to each other [13]. In this case, the size and shape of markers in each section remain unchanged. Changes in coordinates can be described using the following relations:

$$\begin{aligned} x_1 &= x'_0 \times \cos\left(z_1 \frac{\alpha \times \omega}{\vartheta}\right) - y'_0 \times \sin\left(z_1 \frac{\alpha \times \omega}{\vartheta}\right) \\ y_1 &= x'_0 \sin z_1 \frac{\alpha \bullet \omega}{\vartheta} + y'_0 \cos z_1 \frac{\alpha \bullet \omega}{\vartheta} \end{aligned} \quad (2)$$

Here, ϑ and ω are translational and rotational velocities of the die, respectively; x'_0 and y'_0 denote planar coordinates after extrusion, i.e., $x'_0 = x_0 \times (R_1/R_0)$ and $y'_0 = y_0 \times (R_1/R_0)$; α is the slippage parameter representing the fraction of the rotational movement transmitted from the die to the extrudate.

3. Materials and methods

A $\varnothing 12$ mm commercially pure copper cylindrical billet containing five $\varnothing 1.1$ mm A1100 aluminium wires was obtained through direct extrusion. Coordinates of the centre of each marker were $x_0 = [0.5; 1.5; 0; 0; 4]$, $y_0 = [0; 0; 2.5; 3.5; 0]$. HPTE was conducted at room temperature using two sets of parameters: P1 - $\vartheta = 6$ mm/min and $\omega = 1$ rpm, P2 - $\vartheta = 18$ mm/min and $\omega = 1$ rpm. Further details of the extrusion process can be found in [1]. The shape and position of the markers was characterised through X-ray computed tomography using a ZEISS Xradia 520 Versa X-ray microscope operated at 150 kV with the power of 9 W and $10.767 \mu\text{m}$ pixel size. Reconstruction was conducted

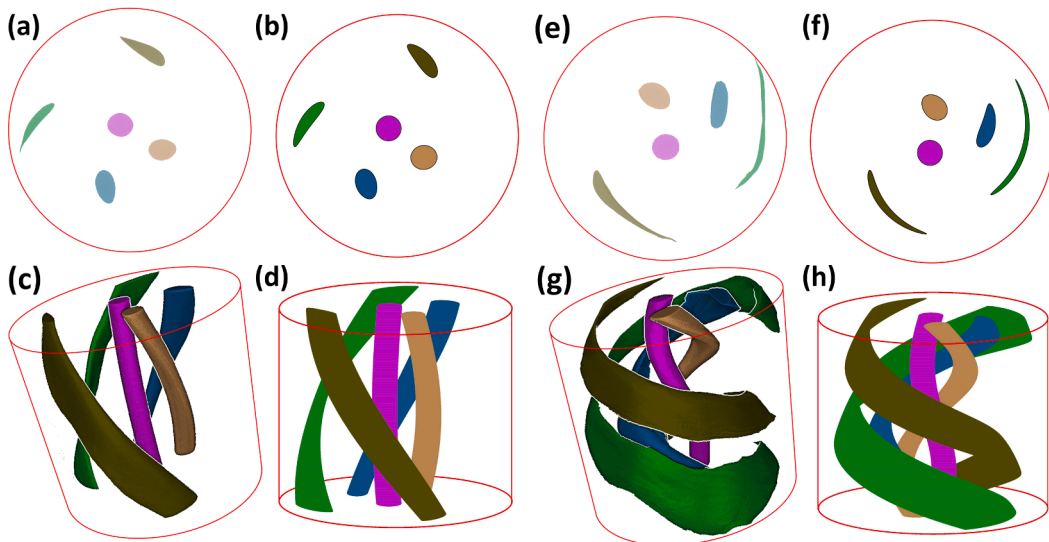


Fig. 2. (a, c, e, g) X-ray computed tomography reconstruction of flow markers after HPTE at 1 rpm die rotational velocity, (b, d, f, h) calculation results Note: extrusion speed (a) to (d) 18 mm/min, (e) to (f) 6 mm/min.

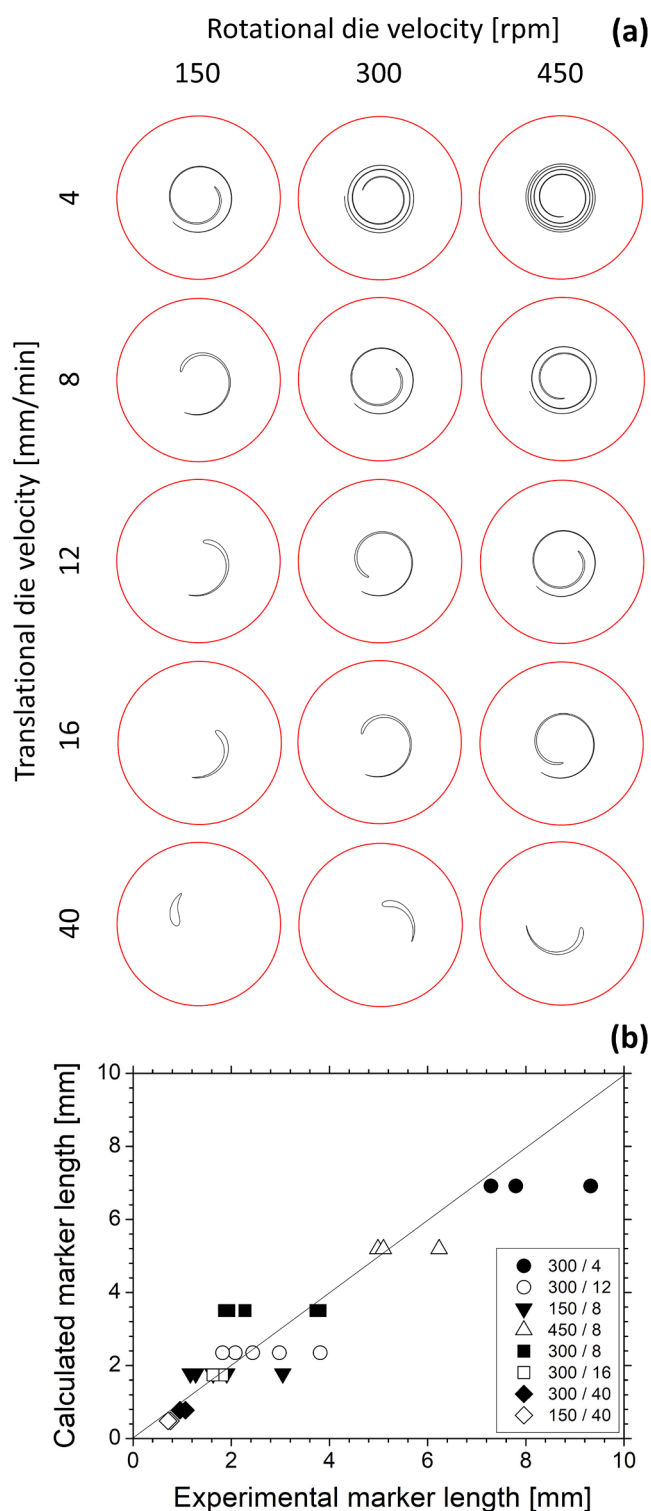


Fig. 3. (a) calculated marker cross-sections after friction stir extrusion, (b) comparison of experimental and calculated marker length.

using Zeiss software, while Drishti software was used for the segmentation and generating final images [14].

4. Results and discussion

Based on the P1 experiment, parameters $z_c = 5.83$ and $n = 3.09$ were obtained using least the least square method to maximise the overlap between calculated and experimental flow markers (Fig. 2(a) and (b)).

Even with the faceted die design, some slippage took place between the dies and the extrudate during extrusion; a slippage parameter $\alpha = 0.6$ was obtained to replicate the twisting of the markers in the reconstructed three-dimensional dataset (Fig. 2(c) and (d)). The geometry of calculated flow markers matched well P2 experiment results thus confirming the efficacy of the proposed method (Fig. 2(e) vs. (f) and (g) vs. (h)).

Only one marker placed at 1/3 of the billet radius was used in the FSE experiments reported in [11]. As the analysis of the marker rotation in three dimensions was not possible based on the reported single two-dimensional section for each combination of process parameters, it was assumed that all of the die rotation was transmitted to the extrudate (i.e., $\alpha = 1$). Fitting parameters $z_c = 1.14$ and $n = 4.57$ were obtained for three specimens extruded at $\omega = 300 \text{ rpm}$, $\vartheta = 8, 12$ and 16 mm/min (Fig. 3(a)). The marker geometry was calculated for the remaining twelve combinations of translational and rotational velocities using the same fitting parameters. Calculated two-dimensional changes in the marker shape matched experimental trends of the increasing marker length with increasing the ratio of rotational to translational velocity. For a quantitative assessment of the efficacy of the proposed method, the values of circumferential strain reported in Fig. 7 of [11] were converted back to the marker length in the circumferential direction. The proposed method provided an accurate estimate of the marker length as shown in Fig. 3(b).

It is worth noting that extrusion experiments with multiple markers combined with the analysis of changes in the position of the markers in different cross-sections would be required to determine the extent of slippage between the extrudate and dies, and to accurately describe the three-dimensional shape of embedded elements.

The study highlights similarities between rotation-assisted extrusion processes. The presented methodology can be further extended in the future to obtain kinematically admissible velocity field for such processes. The method can be used for a quantitative assessment of the extent of mixing of inhomogeneous feedstock for mechanical alloying. Changes in the shape of embedded elements are also important from a standpoint of processing architected materials containing internal helical reinforcements achieved through rotation-assisted extrusion [15].

5. Conclusions

A simple model containing only three adjustable parameters was developed to describe changes in the shape of flow markers during rotation-assisted extrusion. Model parameters were obtained for two processes – HPTE and FSE. The efficacy of the model was tested for process parameters different from those employed to calibrate the model. The model provided an accurate estimate of changes in the geometry of embedded wires.

CRediT authorship contribution statement

Mykola Kulakov: Conceptualization, Visualization, Writing – original draft. **Matthias Mail:** Investigation, Writing – review & editing. **Roman Kulagin:** Conceptualization, Visualization, Methodology, Software, Investigation, Writing – review & editing.

Declaration of Competing Interest

The authors declare that they have no known competing financial interests or personal relationships that could have appeared to influence the work reported in this paper.

References

- [1] Y. Ivanisenko, R. Kulagin, V. Fedorov, A. Mazilkin, T. Scherer, B. Baretzky, H. Hahn, High Pressure Torsion Extrusion as a new severe plastic deformation

- process, Mater. Sci. Eng., A 664 (2016) 247–256, <https://doi.org/10.1016/J.MSEA.2016.04.008>.
- [2] R. Kulagin, Y. Beygelzimer, Y. Estrin, Y. Ivanisenko, B. Baretzky, H. Hahn, A Mathematical Model of Deformation under High Pressure Torsion Extrusion, Metals. 9 (2019), <https://doi.org/10.3390/met9030306>.
- [3] X. Ma, M.R. Barnett, Y.H. Kim, Forward extrusion through steadily rotating conical dies. Part I: experiments, Int. J. Mechan. Sci.. 46 (2004) 449–464, <https://doi.org/10.1016/J.IJMECSCL.2004.03.017>.
- [4] X. Ma, M.R. Barnett, Y.H. Kim, Forward extrusion through steadily rotating conical dies. Part II: theoretical analysis, Int. J. Mechan. Sci. 46 (2004) 465–489, <https://doi.org/10.1016/J.IJMECSCL.2004.03.009>.
- [5] V. Segal, Shear-extrusion method, US Patent 7096705B2, 2006.
- [6] W. Tang, A.P. Reynolds, Production of wire via friction extrusion of aluminum alloy machining chips, J. Mater. Process. Technol. 210 (2010) 2231–2237, <https://doi.org/10.1016/J.JMATPROTEC.2010.08.010>.
- [7] L. Li, V. Gupta, X. Li, A.P. Reynolds, G. Grant, A. Soulami, Meshfree simulation and experimental validation of extreme thermomechanical conditions in friction stir extrusion, Computat. Particle Mechan. (2021), <https://doi.org/10.1007/s40571-021-00445-7>.
- [8] H.S. Valberg, Applied Metal Forming, Cambridge University Press, Cambridge, 2010. Doi: 10.1017/CBO9780511801907.
- [9] J. Kronsteiner, D. Horwatitsch, A. Hinterer, C. Gusenbauer, K. Zeman, Experimental determination of plastic strain in the extrusion process, AIP Conf. Proc. 1769 (2016), 140001, <https://doi.org/10.1063/1.4963538>.
- [10] Y. Beygelzimer, A. Reshetov, S. Synkov, O. Prokof'eva, R. Kulagin, Kinematics of metal flow during twist extrusion investigated with a new experimental method, J. Mater. Process. Technol. 209 (2009) 3650–3656, <https://doi.org/10.1016/J.JMATPROTEC.2008.08.022>.
- [11] X. Li, M.d. Reza-E-Rabby, M. Ryan, G. Grant, A.P. Reynolds, Evaluation of orthogonal strain components in friction extrusion, J. Mater. Res. Technol. 15 (2021) 3357–3364, <https://doi.org/10.1016/J.JMRT.2021.10.001>.
- [12] B. Avitzur, Metal forming: processes and analysis, McGraw-Hill, London, 1968.
- [13] H.G. Grewe, E. Kappler, Über die Ermittlung der Verfestigungskurve durch den Torsionsversuch an zylindrischen Vollstäben und das Verhalten von vielkristallinem Kupfer bei sehr hoher plastischer Schubverformung, Phys. Stat. Solidi (b) 6 (1964) 339–354. <https://doi.org/10.1002/pssb.19640060205>.
- [14] A. Limaye, Drishti: a volume exploration and presentation tool, SPIE Proceedings. 8506 (2012) 191–199, <https://doi.org/10.1117/12.935640>.
- [15] O. Bouaziz, H.S. Kim, Y. Estrin, Architecturing of Metal-Based Composites with Concurrent Nanostructuring: A New Paradigm of Materials Design, Adv. Eng. Mater. 15 (2013) 336–340. <https://doi.org/10.1002/adem.201200261>.